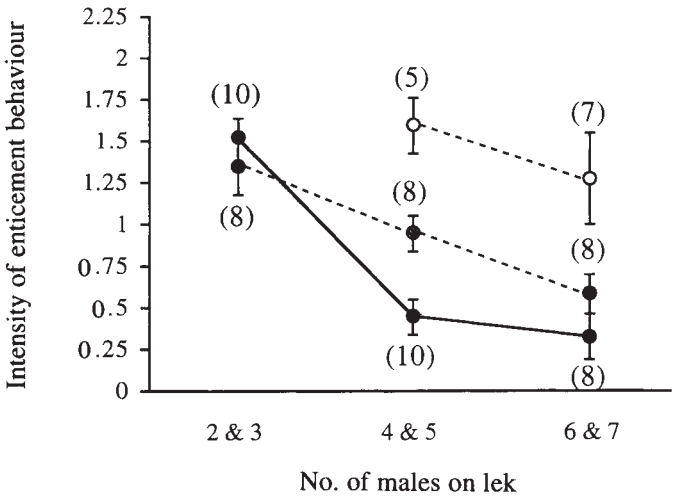

FIG. 4 Observed relationships between mean intensity of enticement behaviour towards flying males and current lek size across males of different rank. The two top-ranking males are represented by black circles, males with rank 3 and 4 are represented by hatched circles, and males of rank 5 and 6 are represented by white circles. The intensity of enticement behaviour to males differed significantly between males of different rank on lek size 4–5 (ANOVA; $F_{2,19}=13.72$, $P<0.0001$) and lek size 6–7 (ANOVA; $F_{2,19}=8.82$, $P<0.01$), but not at lek size 2–3 (ANOVA; $F_{2,17}=3.35$ $P>0.10$). There were no significant differences between the male groups in intensity of enticement behaviour towards flocks containing females at any lek size (ANOVAs; $F_{2,15}<1.73$, $P>0.10$). Male ruffs actively try to entice both females and males to leks by displaying the white underparts of their wings to flying conspecifics. For each enticement event, enticement displays were ranked on a four point scale. Males that did not entice scored as 0, males that flapped their wings while standing scored as 1, males that flapped while jumping up and down scored as 2, and males that hovered over the lek scored as 3. Data come from morning observations within 10 days of the annual population mating peak in 1993; 25 males from 5 different leks were included in the analysis, and the mean enticement intensity for all events present and respective lek size was calculated for each male. Values are means (±s.e.) and numbers in parentheses refer to number of males. Males and lek sizes were grouped to increase the power of the tests, and all observations with females already present on the lek were excluded from the analyses.

tion of some degree of communal displaying, the tight clustering and large aggregations found in most lekking species probably represent the selfish interests of low-ranking males alone.

We suggest that the interaction between lek size and mating skew may be an important factor in promoting aggregated displays, while at the same time setting the upper limit to lek size. In combination with female preferences for traditional lek sites in areas of suitable breeding habitat, this could be an important component in the explanation of the evolution of lekking. Further empirical data suggest that the patterns we have observed in the ruff are common to several other species of lekking birds and mammals (F.W. and I.P.F.O., manuscript in preparation), and the suggested mechanism for the evolution of aggregated displays, therefore, appears to be general. Future studies should focus on both degree of male mating skew and copulation rates, when discussing how individual males should distribute themselves. □

Received 24 June; accepted 24 November 1994.

1. Bradbury, J. W. in *Natural Selection and Social Behaviour* (eds Alexander, R. D. & Tinkle, D. W.) 138–169 (Chiron, New York, 1981).
2. Bradbury, J. W. & Gibson, R. M. in *Mate Choice* (ed. Bateson, P.) 109–138 (Cambridge Univ. Press, 1983).
3. Bradbury, J. *et al. Anim. Behav.* **34,** 1694–1709 (1986).
4. Beehler, B. M. & Foster, M. S. *Am. Nat.* **131,** 203–219 (1988).
5. Alatalo, R. V. *et al. Behav. Ecol.* **3,** 53–59 (1992).
6. Clutton-Brock, T. H. *et al. Behav. Ecol.* **3,** 234–243 (1992).
7. Höglund, J. *et al. Behav. Ecol. Sociobiol.* **32,** 31–39 (1993).
8. Stillman, R. A. *et al. Behav. Ecol.* **4,** 1–6 (1993).
9. Davies, N. B. in *Behavioural Ecology* (eds Krebs, J. R. & Davies, N. B.) 263–294 (Blackwell, Oxford, 1991).
10. Wiley, R. H. *Adv. Study Behav.* **20,** 202–291 (1991).
11. Milinski, M. & Parker, G. A. in *Behavioural Ecology* (eds Krebs, J. R. & Davies, N. B.) 137–168 (Blackwell, Oxford, 1991).
12. Hogan-Waarburg, A. J. *Ardea* **54,** 8–229 (1966).
13. Lank, D. B. & Smith, C. M. *Behav. Ecol. Sociobiol.* **30,** 323–329 (1992).
14. van Rhijn, J. G. *The Ruff* (Poyser, London, 1991).
15. Keller, L. & Vargo, E. L. in *Queen Number and Sociality in Insects*. (ed. Keller, L.). 16–44 (Oxford Univ. Press, 1993).
16. Reeve, H. K. & Ratnicks, F. L. W. in *Queen Number and Sociality in insects*. (ed. Keller, L.), 45–85 (Oxford Univ. Press, 1993).

ACKNOWLEDGEMENTS. We thank S. Albon, J. Höglund, A. P. Møller and S. Ulfstrand for helpful comments on an earlier draft. S. Albon also kindly helped with the statistical analyses. This paper was written while F.W. was visiting the Institute of Zoology, London, on a Royal Swedish Academy of Sciences grant. The field work was funded by RSAS and WWF grants to F.W. and I.P.F.O. was supported by a NERC Postdoctoral Fellowship.

Reduced hippocampal LTP and spatial learning in mice lacking NMDA receptor ε1 subunit

Kenji Sakimura*, Tatsuya Kutsuwada*, Isao Ito†, Toshiya Manabe‡, Chitoshi Takayama§, Etsuko Kushiya*, Takeshi Yagi‖¶, Shinichi Aizawa‖¶, Yoshiro Inoue§, Hiroyuki Sugiyama† & Masayoshi Mishina*#☆

* Department of Neuropharmacology, Brain Research Institute, Niigata University, Niigata 951, Japan
† Department of Biology, Faculty of Science, Kyushu University, Fukuoka 812, Japan
‡ Department of Neurophysiology, Institute for Brain Research, Faculty of Medicine, University of Tokyo, Tokyo 113, Japan
§ Department of Anatomy, Hokkaido University School of Medicine, Sapporo 060, Japan
‖ Laboratory of Molecular Oncology, Tsukuba Life Science Center, Institute of Physical and Chemical Research, Ibaraki 305, Japan
Department of Pharmacology, Faculty of Medicine, University of Tokyo, Tokyo 113, Japan

THE NMDA (*N*-methyl-D-aspartate) receptor channel is important for synaptic plasticity, which is thought to underlie learning, memory and development[1,2]. The NMDA receptor channel is formed by at least two members of the glutamate receptor (GluR) channel subunit families, the GluRε (NR2) and GluRζ (NR1) subunit families[3–8]. The four ε subunits are distinct in distribution, properties and regulation[5–14]. On the basis of the Mg^{2+} sensitivity and expression patterns, we have proposed that the ε1 (NR2A) and ε2 (NR2B) subunits play a role in synaptic plasticity[6,14]. Here we show that targeted disruption of the mouse ε1 subunit gene resulted in significant reduction of the NMDA receptor channel current and long-term potentiation at the hippocampal CA1 synapses. The mutant mice also showed a moderate deficiency in spatial learning. These results support the notion that the NMDA receptor channel-dependent synaptic plasticity is the cellular basis of certain forms of learning.

To disrupt the GluRε1 locus, the targeting vector shown in Fig. 1*a* was transfected into murine TT2 embryonic stem (ES) cells[15]. Two targeted clones transmitted the mutation through the germ line, and their progenies were analysed by Southern blot hybridization (Fig. 1*b*). Homozygous GluRε1 mutant mice

¶ Present addresses; Laboratory of Neurobiology and Behavioral Genetics, National Institute for Physiological Sciences, Okazaki 444, Japan (T.Y.) and Laboratory of Morphogenesis, Institute of Molecular Embryology and Genetics, Kumamoto University School of Medicine, Kumamoto 860, Japan (S.A.).
☆ To whom correspondence should be addressed at the Department of Pharmacology, Faculty of Medicine, University of Tokyo, Hongo 7-3-1, Bunkyo-ku, Tokyo 113, Japan.

developed and mated normally, in contrast to the lethal effect of disruption of the GluRζ1 (NR1) gene[16]. The mutant mice seemed to be 'jumpy'. *In situ* hybridization analysis of the sagittal brain sections with oligonucleotide probes corresponding to the disrupted (probe ε1C) and intact (probe ε1A) regions showed that normal GluRε1-RNA transcripts were absent in mutant mice (Fig. 1*c*). Expression of messenger RNAs corresponding to the other NMDA receptor channel subunits were not appreciably affected by the GluRε1 disruption. Western blot analysis of forebrain proteins showed that the mutant mice (−/−) contained no detectable GluRε1 protein (M_r 175K), and the content of the heterozyous mice (+/−) was approximately half that of the wild-type mice (+/+), whereas the contents of GluRε2 protein (180K) and the large myelin-associated glycoprotein (LMAG) were not appreciably affected by the mutation (Fig. 1*d*).

Histological examination of various brain regions where the ε1 subunit mRNA was abundantly expressed, such as the hippocampal formation, cerebral cortex, olfactory bulb, ventral posterior nucleus of the thalamus, spinal tract nucleus of trigeminal nerve and inferior olive[5,7,9,10] showed no obvious morphological abnormalities in the GluRε1-mutant mice (Fig. 2) The ε1 subunit mRNA is expressed only postnatally[9] and thus may exert little effect on development.

Efficacy of excitatory transmission in the hippocampal CA1 pyramidal neurons, estimated by input–output relationships of field excitatory postsynaptic potentials (e.p.s.ps), was indistinguishable between the wild-type and mutant slices, and the time courses of the field potential responses were also similar (Fig. 3*a*). No significant difference in the extent of paired-pulse facilitation was found between the wild-type (1.75 ± 0.04, mean ±s.e.m., $n = 10$) and mutant (1.67 ± 0.03, $n = 10$) slices. But NMDA receptor channel currents, expressed as the ratio to 6-cyano-7-nitroquinoxaline-2,3-dione (CNQX)-sensitive non-NMDA receptor channel currents, were significantly reduced in the mutant slices (19 ± 3%, $n = 5$) compared with the wild-type slices (43 ± 6%, $n = 5$) (*t*-test, $P < 0.01$) (Fig. 3*b*). On the other hand, there was no significant difference in the current–voltage relationship of the NMDA receptor channel currents (Fig. 3*c*), and the reversal potential in the mutant slices (2 ± 1 mV, $n = 7$) was similar to that in the wild-type slices (3 ± 2 mV, $n = 6$).

Tetanic stimulation caused a long-lasting increase in the synaptic strength in the wild-type slices; the relative e.p.s.p. slope 60 min after tetanic stimulation being 187 ± 8% of the average slope before stimulation ($n = 20$) (Fig. 3*d*). But the extent of the long-lasting potentiation was significantly decreased in the mutant slices (126 ± 6%, $n = 17$) ($P < 0.01$). In mutant mice defective in the γ isoform of protein kinase C (PKCγ), an apparent defect in hippocampal long-term potentiation (LTP) was fully removed when low-frequency stimulation was applied before tetanic stimulation[17]. The extent of potentiation induced by tetanic stimulation after low-frequency stimulation was still significantly smaller in the mutant mice (162 ± 15%, $n = 8$) than in the wild-type mice (209 ± 15%, $n = 8$) ($P < 0.05$) (Fig. 3*e*).

As a control for the Morris water-maze task[18], mice were first tested on a visible-platform task. Although the mutant mice took

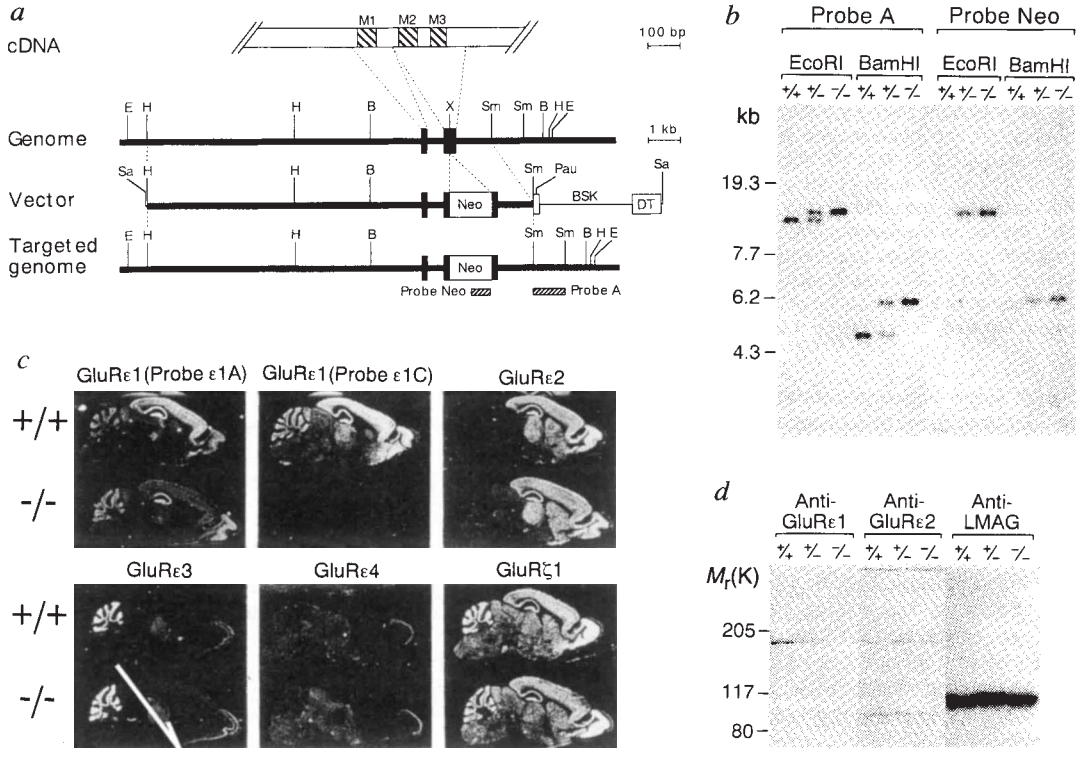

FIG. 1 Targeted disruption of the mouse NMDA receptor channel ε1 subunit gene. *a*, Schematic representations of GluRε1 complementary DNA, genomic DNA, targeting vector and disrupted gene. M1–3, putative transmembrane segments; Neo, neomycin resistant gene; Pau, mRNA-destabilizing and transcription-pausing signals[25]; BSK, plasmid pBluescript; DT, diphtheria toxin gene; B, *Bam*HI; E, *Eco*RI; H, *Hin*dIII; Sa, *Sal*I; Sm, *Sma*I; X, *Xcm*I. *b*, Southern blot analysis of *Eco*RI- or *Bam*HI-digested genomic DNA. *c*, *In situ* hybridization analysis of parasagittal brain sections. *d*, Western blot analysis of forebrain proteins with anti-GluRε1, anti-GluRε2 and anti-LMAG antibodies. METHODS. The targeting vector pTVGRε1 was constructed by inserting the 1.3-kilobase (kb) blunted *Eco*RI–*Bam*HI fragment from pGK2Neo containing the neomycin phosphotransferase gene driven by the phosphoglycerate kinase promoter[25] into the blunted *Xcm*I site of 10-kb GluRε1 genomic DNA isolated from a C57BL/6 genomic library (provided by A. Shimizu) and by ligating pPauDT1 for negative selection, a derivative of pHFZprNeoDT[25], in which the multi-cloning sequence between the *Cla*I and *Sac*I sites was removed and a synthetic adapter carrying *Sal*I, *Hin*dIII and *Sma*I sites replaced the 16.5-kb *Not*I–*Xho*I segment. TT2 (C57BL/6 × CBA F_1 hybrid) ES cells[15] were transfected by *Not*I-digested pTVGRε1, and five targeted clones were identified by G418 selection, polymerase chain reaction and Southern blot hybridization, the frequency being 0.4% of G418-resistant clones. Chimaeras produced by injection of these cells into 8-cell embryos of ICR mice were mated with C57BL/6 mice and clones H10 and N6 transmitted the mutation through the germ line. The contribution of the ε1 subunit is larger in adult animals[9], thus all analyses were done with mature mice (9–10 weeks old), using wild-type littermates as controls. Essentially the same results were obtained with two lines and data from H10 are shown. *In situ* hybridization and western blot analyses were done as described[9,10,26]. Oligonucleotide probe ε1C is complementary to the nucleotide residues 1,795 to 1,839 of the ε1 subunit cDNA[5]. Anti-GluRε1 and anti-GluRε2 antibodies were prepared using fusion proteins of a carboxy-terminal portion of the ε1 (amino-acid residues 1,335 to 1,414)[5] or ε2 subunit (residues 1,353 to 1,432)[6] with glutathione-*S*-transferase[26]. Anti-LMAG antibody provided by T. Inuzuka.

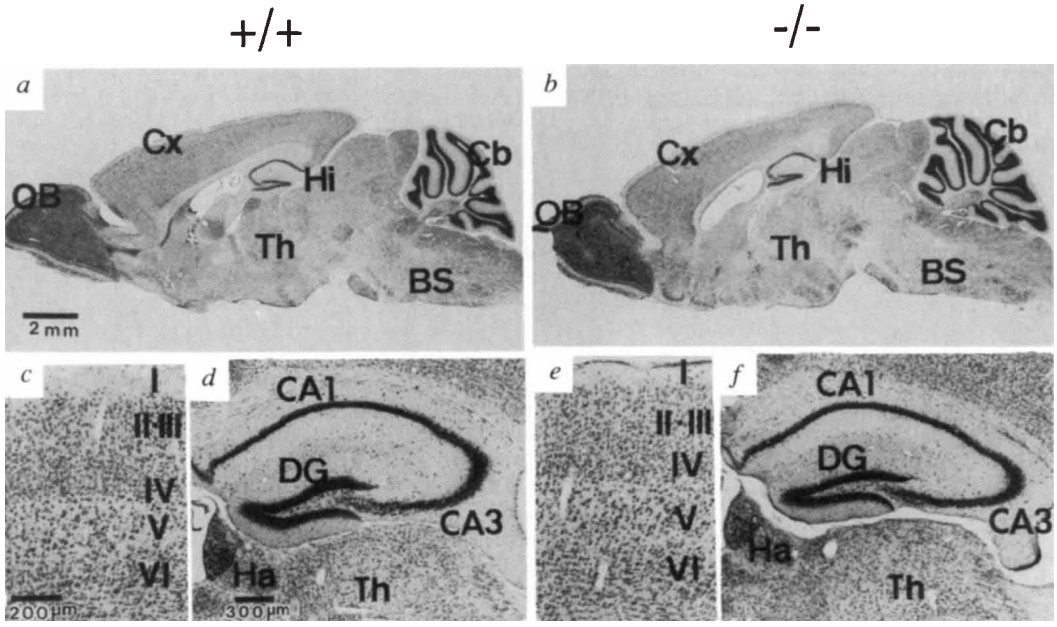

FIG. 2 Nissl-stained brain sections of the wild-type (+/+) (*a*, *c*, *d*) and mutant (−/−) (*b*, *e*, *f*) mice. *a*, *b*, Para-sagittal sections of the whole brain. *c*, *e*, Coronal sections of the parietal lobe. *d*, *f*, Coronal sections of the hippocampal formation. Mice were fixed by transcardial perfusion with 4% paraformaldehyde in 0.1 M phosphate buffer, pH 7.4. Cryostat-prepared 20-μm sections were stained with toluidine blue. BS, Brainstem; CA1 and CA3 are fields of the Ammon's horn; Cb, cerebellum; Cx, cerebral cortex; DG, dentate gyrus; Ha, habenular nucleus; Hi, hippocampal formation; OB, olfactory bulb; Th, thalamus; I–VI, cortical laminae I–VI.

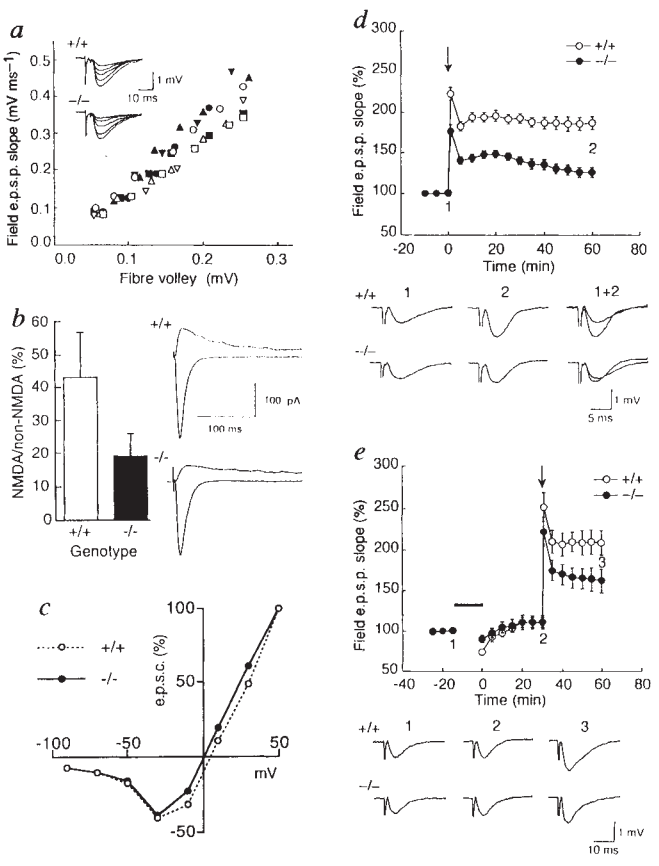

FIG. 3 Synaptic responses in hippocampal CA1 pyramidal cells of the wild-type (open symbols) and mutant (filled symbols) mice. *a*, Initial slopes of field e.p.s.ps as a function of presynaptic fibre volley amplitudes. Each symbol represents a set of experiments from a single slice. Inset traces show typical field e.p.s.ps obtained with various stimulus intensities. *b*, Ratios of peak NMDA receptor channel currents at +40 mV to peak synaptic currents at −90 mV, measured with the whole-cell voltage-clamp recording. The NMDA receptor-mediated current recorded at +40 mV was blocked by 25 μM D-APV. Upper traces show synaptic currents at +40 mV in the presence of 20 μM CNQX, and lower traces currents at −90 mV in the control solution. Ratios of the two currents in the wild-type and mutant slices measured with the intracellular recording under discontinuous voltage-clamp were 34 ± 11% and 12 ± 3% ($n = 6$ each), respectively, at −40 mV holding potential. *c*, Representative current–voltage relationships of NMDA receptor channel currents measured in the presence of 20 μM CNQX. The currents were normalized to the values at +50 mV e.p.s.c., excitatory post-synaptic current. *d*, *e*, LTP of the hippocampal CA1 field e.p.s.p. expressed as percentage of the mean before tetanic stimulation. The control stimulation intensity was ~30% of the maximal response and it was kept constant throughout the experiment. A single slice was used from one animal. *d*, Potentiation induced by tetanic stimulation (100 Hz for 1 s, 2 trains, 30-s interval, arrow) in 20 wild-type slices (open circles) and 17 mutant slices (filled circles). *e*, Effect of previous low-frequency stimulation (1 Hz for 900 s, thick bar) on potentiation induced by tetanic stimulation (100 Hz for 1 s, arrow); eight slices each from the wild-type (open circles) and mutant (filled circles) mice. Typical traces (average of three recordings) at the times indicated by Arabic numerals are shown below.

METHODS. The series of experiments included some performed blind (47%) and essentially the same results were obtained. Transverse hippocampal slices (~400 μm) were placed in a submerged recording chamber perfused continuously with artificial cerebrospinal fluid (ACSF) equilibrated with 95% O_2/5% CO_2 at 32 ± 0.5 °C at a rate of 3–4 ml min^{-1}. Extracellular field e.p.s.ps were recorded with an electrode filled with 0.9% (NaCl in CA1 stratum radiatum[27]. A bipolar tungsten electrode was used to stimulate Schaffer collateral/commissural afferents ~200 μm away from the recording electrode. Stimulus duration, 80 μs. For measurements of paired-pulse facilitation, paired pulses were given at 40 ms intervals. ACSF contained 119 mM NaCl, 2.5 mM KCl, 2.5 mM $CaCl_2$, 1.3 mM $MgSO_4$, 1 mM NaH_2PO_4, 26 mM $NaHCO_3$ and 10 mM glucose. E.p.s.cs were recorded from CA1 pyramidal cells with a patch electrode (3–6 MΩ) in the whole-cell voltage-clamp mode (Axopatch 1D) using the 'blind' technique[28,29]. The pipette solution contained 122.5 mM caesium gluconate, 17.5 mM CsCl, 10 mM HEPES buffer, 0.2 mM EGTA, 8 mM NaCl, 2 mM Mg–ATP, 0.3 mM Na_3–GTP (pH 7.2, 290–300 mOsm). The values of the membrane potential were corrected for the liquid-junction potential at the electrode tip. The discontinuous voltage clamp (holding potential, −40 mV; sampling clock, 1–2 kHz) was used to record e.p.s.cs at 25 ± 5 °C with an intracellular electrode (30–40 MΩ) filled with 3 M CsCl. Picrotoxin (50–100 μM) was present in all experiments.

longer to reach the platform on the first block of trials, they subsequently performed as efficiently as the wild-type mice (Fig. 4*a*). Thus, the GluRε1-mutant and wild-type mice are able to perform the non-spatial learning water-maze task. In the hidden-platform task, the wild-type mice quickly learned to locate the hidden platform, whereas the mutant mice took significantly longer (Fig. 4*b*).

In the transfer test[2], the wild-type mice spent longer in the trained quadrant than in the opposite, right or left quadrant (Fig. 4*c*), and crossed the exact spot where the platform had been located more often than they did equivalent locations in other quadrants (Fig. 4*d*). The mutant mice also searched preferentially in the trained quadrant, but not as selectively as the wild-type mice; the difference in searching time between the trained and right quadrants was less significant. The searching time in the trained quadrant by the mutant mice was significantly shorter than by the wild-type mice ($P<0.01$). Furthermore, the mutant mice failed to cross the trained site selectively; there was no significant difference in the number of times that they cross the trained site compared with the equivalent location in the right-hand quadrant. The mutant mice crossed the trained spot less often than the wild-type mice ($P<0.01$). These results suggest that the GluRε1-mutant mice perform the spatial learning task less precisely than the wild-type mice.

Through the analyses of expression patterns and functional properties of diverse NMDA receptor channel subunits identified by molecular cloning, we have proposed that of the four ε subunits, the ε1 and ε2 subunits are involved in synaptic plasticity[6,14]. Here we have provided experimental evidence that the ε1 subunit is a component of functional NMDA receptor channels in the hippocampus and is important for LTP of synaptic transmission and spatial learning. Because Ca^{2+} entry through NMDA receptor channels triggers the induction of LTP in the hippocampal CA1 region[1], the decrease in NMDA receptor channel activity should causally relate to the reduction of LTP in the GluRε1 mutant mice. The observation that hippocampal LTP is not completely abolished by the deprivation of the ε1 subunit implies that the ε2 subunit would also play a role in the hippocampal LTP, as both the ε1 and ε2 subunit mRNAs are expressed in the adult hippocampus[5,6,9,10] and share similar functional properties such as high sensitivity to Mg^{2+} blockage and modulation[5,7,11,13]. The GluRε1-mutant mice are apparently jumpy and seem to have enhanced startle response, similar to mutant mice defective in α isoform of Ca^{2+}-calmodulin-dependent protein kinase II (α-CaMKII)[19]. It is possible that disturbance of LTP in amygdala for example, might be related to the behaviour[19].

Synaptic plasticity, represented by LTP in the hippocampus, has long been thought to underlie learning and memory[1], but experimental evidence for the linkage is limited. The initial approach demonstrated that chronic intraventricular infusion of 2-amino-5-phosphonovalerate (APV), an antagonist of the NMDA receptor channel, impaired both hippocampal LTP and spatial learning in rat[2,20]. We have shown by gene targeting that the GluRε1-mutant mice, showing reduced hippocampal LTP, have a moderate defect in spatial learning, which is quantitatively similar to results obtained with an intermediate dose of APV (ref. 20), supporting the notion that the NMDA receptor channel-dependent synaptic plasticity is the cellular basis of certain forms of learning. But it cannot be excluded that possible disturbance of synaptic transmission, undetected slight abnormalities of the brain organization or the jumpy behaviour of the GluRε1-mutant mice might affect the observed deficiency in spatial learning. Mice defective in α-CaMKII or the non-receptor tyrosine kinase *fyn*, showed a deficiency in hippocampal LTP and spatial learning, though the exact mechanisms were unknown[19,21,22]. These effects may be indirect because in *fyn*-mutant mice, defects were noted in the arrangement of hippocampal neurons and myelination[21,23]. PKCγ-mutant mice showed spatial learning capabilities in spite of an apparent defect in hippocampal LTP[17,24], and LTP could be fully induced in these mice when low-frequency stimulation was applied before tetanic stimulation. In the GluRε1-mutant mice, LTP was significantly reduced even after such stimulation. Our findings taken together are in line with the notion that synaptic plasticity is the cellular mechanism of certain forms of memory and learning. □

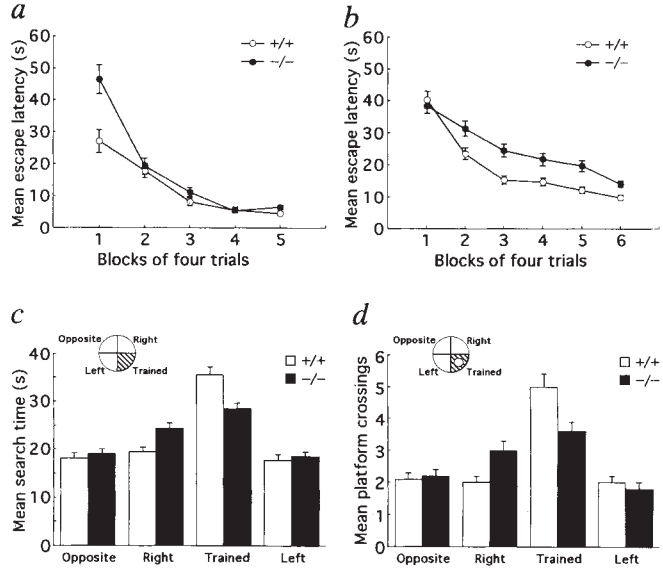

FIG. 4 Performance in the Morris water maze tasks by the wild-type (open symbols) and mutant (filled symbols) mice. *a*, Escape latency in the visible-platform test ($n=16$, each). Analysis of variance (ANOVA) with repeated measures showed significant effects of genotypes ($F_{(1,30)}=11.71$, $P<0.01$) and trial blocks ($F_{(4,120)}=78.74$, $P<0.01$). The interaction between trial blocks and genotypes ($F_{(4,120)}=7.24$, $P<0.01$) was significant only at the first block ($F_{(1,30)}=11.51$, $P<0.01$). *b*, Escape latency in the hidden-platform test ($n=40$, each). The effects of genotypes ($F_{(1,78)}=12.03$, $P<0.01$) and trial blocks ($F_{(5,390)}=53.89$, $P<0.01$) were significant, and there was no interaction. There was no significant difference in body weight and swimming speed between the wild-type (21.10 ± 0.46 g and 24.27 ± 0.33 cm s^{-1}, respectively) and mutant (20.96 ± 0.40 g and 24.22 ± 0.31 cm s^{-1}, respectively) mice. *c*, *d*, Performance in the transfer test ($n=40$, each), on the day after hidden-platform training. *c*, Quadrant search time. The wild-type mice spent more time in the trained than in the other three quadrants; ANOVA, $F_{(2,156)}=67.15$, $P<0.01$; Tukey analysis, trained quadrant > other quadrants, $P<0.01$. Mutant mice also spent more time in the trained quadrant; $F_{(2,156)}=30.57$, $P<0.01$; Tukey analysis, trained > opposite and left, $P<0.01$, trained > right, $P<0.05$. *d*, Number of crossings. The wild-type mice crossed the trained site more often than equivalent sites in other quadrants; $F_{(3,156)}=26.12$, $P<0.01$; Tukey analysis, trained > others, $P<0.01$. Mutant mice failed to cross the trained site selectively; $F_{(3,156)}=9.84$, $P<0.01$; Tukey analysis, trained = right, trained > opposite and left, $P<0.01$.

METHODS. The visible- and hidden-platform tests were done as described[21,30] with slight modifications. The series of experiments included 63% performed blind and essentially the same results were obtained. The training apparatus was a circular white-painted steel pool, 120 cm in diameter. The water was made opaque by adding skimmed milk and was kept at 18.5 ± 0.5 °C. Before the test, mice were first trained to swim and climb on the platform. In the visible-platform test, mice were given one block of four trials on the first day and two blocks of trials on the second and third days. In the hidden-platform test, mice were given one trial of the visible-platform task as pretraining one day before the test and were given one block of four trials per day for six consecutive days. Swimming paths were tracked with a camera and stored in a computer (TARGET/2 system, Neuroscience Inc., Tokyo).

Received 27 July; accepted 22 November 1994.

1. Bliss, T. V. P. & Collingridge, G. L. *Nature* **361,** 31–39 (1993).
2. Morris, R. G. M., Anderson, E., Lynch, G. S. & Baudry, M. *Nature* **319,** 774–776 (1986).
3. Moriyoshi, K. *et al. Nature* **354,** 31–37 (1991).
4. Yamazaki, M. *et al. FEBS Lett.* **300,** 39–45 (1992).
5. Meguro, H. *et al. Nature* **357,** 70–74 (1992).
6. Kutsuwada, T. *et al. Nature* **358,** 36–41 (1992).
7. Monyer, H. *et al. Science* **256,** 1217–1221 (1992).
8. Ikeda, K. *et al. FEBS Lett.* **313,** 34–38 (1992).
9. Watanabe, M., Inoue, Y., Sakimura, K. & Mishina, M. *NeuroReport* **3,** 1138–1140 (1992).
10. Watanabe, M., Inoue, Y., Sakimura, K. & Mishina, M. *J. comp. Neurol.* **338,** 337–390 (1993).
11. Mori, H., Yamakura, T., Masaki, H. & Mishina, M. *NeuroReport* **4,** 519–522 (1993).
12. Ishii, T. *et al. J. biol. Chem.* **268,** 2836–2843 (1993).
13. Monyer, H., Burnashev, N., Laurie, D. J., Sakmann, B. & Seeburg, P. H. *Neuron* **12,** 529–540 (1994).
14. Mishina, M. *et al. Ann. N.Y. Acad. Sci.* **707,** 136–152 (1993).
15. Yagi, T. *et al. Analyt. Biochem.* **214,** 70–76 (1993).
16. Li, Y. *et al. Cell* **76,** 427–437 (1994).
17. Abeliovich, A. *et al. Cell* **75,** 1253–1262 (1993).
18. Morris, R. G. M. *Learn. Motiv.* **12,** 239–260 (1981).
19. Silva, A. J., Stevens, C. F., Tonegawa, S. & Wang, Y. *Science* **257,** 201–206 (1992).
20. Davis, S., Butcher, S. P. & Morris, R. G. M. *J. Neurosci.* **12,** 21–34 (1992).
21. Silva, A. J., Paylor, R., Wehner, J. M. & Tonegawa, S. *Science* **257,** 206–211 (1992).
22. Grant, S. G. N. *et al. Science* **258,** 1903–1910 (1992).
23. Umemori, H., Sato, S., Yagi, T., Aizawa, S. & Yamamoto, T. *Nature* **367,** 572–576 (1994).
24. Abeliovich, A. *et al. Cell* **75,** 1263–1271 (1993).
25. Yagi, T. *et al. Analyt. Biochem.* **214,** 77–86 (1993).
26. Araki, K. *et al. Biochem. biophys. Res. Commun.* **197,** 1267–1276 (1993).
27. Ito, I. & Sugiyama, H. *NeuroReport* **2,** 333–336 (1991).
28. Blanton, M. G., Lo Turco, J. J. & Kriegstein, A. R. *J. Neurosci. Meth.* **30,** 203–210 (1989).
29. Coleman, P. A. & Miller, R. F. *J. Neurophysiol.* **61,** 218–230 (1989).
30. Zhang, Y., Saito, H. & Nishiyama, N. *Brain Res.* **658,** 127–134 (1994).

ACKNOWLEDGEMENTS. The first two authors contributed equally to the work. We thank R. Natsume for assistance in animal care and DNA analyses, N. Takeda for help in the preparation of chimaeric mice, H. Saito and N. Nishiyama for advice on the water maze task, M. Nakazawa for advice on statistical analyses, A. Shimizu for a mouse genomic DNA library, T. Inuzuka for anti-LMAG antibody, and H. Niki and T. Takahashi for critically reading the manuscript. This investigation was supported by the Ministry of Education, Science and Culture of Japan, the Uehara Memorial Foundation, the Ministry of Health and Welfare of Japan, the Naito Foundation and the Yamanouchi Foundation.

Subthreshold synaptic Ca^{2+} signalling in fine dendrites and spines of cerebellar Purkinje neurons

Jens Eilers, George J. Augustine* & Arthur Konnerth†

I. Physiologisches Institut der Universität des Saarlandes, D-66421 Homburg, Germany
* Department of Neurobiology, Duke University Medical Center, Durham, North Carolina 27710, USA

THE conventional view of synaptic integration is that it results from the simple summation of electrical signals produced by each active synapse innervating a given neuron[1]. However, because synaptic action can go beyond the production of postsynaptic electrical signals, to include intracellular biochemical events such as the generation of second messengers, it is possible that synaptic integration could occur at another level[2]. We have considered this possibility by examining changes in the dendritic concentration of the second messenger, calcium, resulting from subthreshold excitatory synaptic activity in cerebellar Purkinje neurons. We report here clear evidence that such non-electrical synaptic integration occurs and that it takes place in restricted dendritic compartments consisting of spines and adjacent fine dendrites.

By combining whole-cell patch-clamp recordings with confocal laser scanning microscopy (Fig. 1*a*) we could measure postsynaptic Ca^{2+} signals from the finest, terminal spiny dendrites of single Purkinje neurons of cerebellar slices (Figs 1*b* and 2). Activation of excitatory, parallel fibre (PF) synapses produced multiple types of dendritic Ca^{2+} changes. Single-shock activation of a sufficient number of PF synapses to produce a subthreshold excitatory postsynaptic potential (e.p.s.p.), as in Fig. 1*c*, produced highly localized but clearly visible rises in postsynaptic Ca^{2+} activity (Fig. 1*d*). Such Ca^{2+} signals were readily found in all Purkinje neurons that were tested ($n=37$). These rises in postsynaptic Ca^{2+} concentration occurred at levels of synaptic activity that were below the threshold for regenerative electrical activity, such as action or plateau potentials[3]. Stimulation of a larger number of PFs, a number sufficient to reach the threshold for producing a propagated action potential (the so-called 'simple spike'), also produced a rise in postsynaptic Ca^{2+} concentration that was quite similar to that produced by subthreshold e.p.s.ps (Fig. 1*e*,*f*). These Ca^{2+} signals were confined to the same compartment of terminal spiny dendrites, but resulted in larger rises in postsynaptic Ca^{2+} concentration within the activated compartment. Still stronger and repetitive stimulation caused Ca^{2+} changes that extended beyond spiny dendrites and included tertiary and secondary dendrites, confirming previous observations[4,5]. Even larger e.p.s.ps, sufficient to activate dendritic Ca^{2+} spikes[5,9], produced very large Ca^{2+} signals throughout the Purkinje neuron[5] (data not shown).

The postsynaptic Ca^{2+} signals resulting from subthreshold PF synaptic activity were not restricted to individual dendrites or spines, but instead appeared in a restricted area consisting of both (Fig. 2). In the example shown in Fig. 2, a single subthreshold PF-e.p.s.p. produced rises in Ca^{2+} concentration in spines (trace 1) as well as in the larger dendritic structure to which these spines were attached (trace 3). This was a general finding, with the dendritic Ca^{2+} signals usually found to terminate abruptly within the dendrites, over distances of just a few micrometres. The spatial extent of these postsynaptic Ca^{2+} signals may be limited by the failure of the electrical signals to propagate beyond the points at which the dendrites branch within the dendritic arborization. The fact that these Ca^{2+} signals are not restricted to the dendritic spines, where the PF terminals contact the Purkinje neurons[10], contrasts with the case of hippocampal CA3 pyramidal neurons, where NMDA receptor-mediated postsynaptic Ca^{2+} influx is localized to single dendritic spines[11]. However, the spread of Ca^{2+} signals into both spines and dendrites is not an artefact resulting from optical blurring of signals emanating from only one of these structures, because extracellular regions immediately adjacent to dendritic spines showed no significant changes in fluorescence during synaptic activity (Fig. 2, trace 2). Further, the time courses of the postsynaptic Ca^{2+} signals produced by PF-e.p.s.ps appeared similar in both dendrites and their spines (Fig. 2). There was no detectable lag in the rise of the Ca^{2+} signals in these two compartments within the 33 ms time resolution of our imaging method. Thus, the presence of Ca^{2+} signals both in spines and in adjacent dendrites results from the fact that Ca^{2+} rises in both compartments. These results indicate that the subthreshold postsynaptic Ca^{2+} signals of Purkinje neurons are not restricted to dendritic spines and, in fact, the spines may not even be the initial source of the Ca^{2+} influx that produces these signals.

These Ca^{2+} signals were quite transient within both compartments, declining to half their maximum amplitude in less than 2 s (Fig. 2). This is an upper estimate of the time course of the Ca^{2+} signals, which could be even more rapid[3,5] because of the Ca^{2+}-buffering properties of the fluorescent indicator[12,13]. This brief time course also contrasts with the case of dendritic spines in hippocampal CA3 pyramidal neurons[11] but is much like the case for NMDA receptor-mediated postsynaptic Ca^{2+} signals in cerebral cortex[14] and in hippocampal CA1 neurons[15].

We next examined the sources of Ca^{2+} that produce the postsynaptic signals. These signals require activation of postsynaptic α-amino-3-hydroxy-5-methyl-4-isoxazole propionic acid (AMPA) receptors because a blocker of these receptors, 6-cy-

† To whom correspondence should be addressed.